MEDICAL SCIENCE MONITOR

ANIMAL STUDY

e-ISSN 1643-3750
© Med Sci Monit, 2017; 23: 1099-1105
DOI: 10.12659/MSM.903292

Received: 2017.01.11
Accepted: 2017.02.01
Published: 2017.03.02

Mechanical Stimulus-Induced Withdrawal Behavior Increases Subsequent Pre-Stimulus Local Field Potential Power in the Rostral Anterior Cingulate Cortex in Unanesthetized Rats

Authors' Contribution:
Study Design A
Data Collection B
Statistical Analysis C
Data Interpretation D
Manuscript Preparation E
Literature Search F
Funds Collection G

AE Zui Shen
B Jing Sun
B Boyi Liu
C Yongliang Jiang
D Yuanyuan Wu
F Jialing Wang
DG Xiaomei Shao
AE Jianqiao Fang

Department of Neurobiology and Acupuncture Research, The 3rd Clinical College, Zhejiang Chinese Medical University, Hangzhou, Zhejiang, P.R. China

Corresponding Authors: Jianqiao Fang, e-mail: fangjianqiao7532@163.com, Xiaomei Shao, e-mail: 13185097375@163.com
Source of support: This study was supported by the National Natural Science Foundation of China (81574056), the Zhejiang Provincial Natural Science Foundation of China (LY15H270009), the Key Science and Technology Innovation Team of Zhejiang Province (2013TD15), the Project Supported by Zhejiang Province Top Key Discipline of Chinese Medicine-Acupuncture and Tuina, Special Financial Grant from the China Postdoctoral Science Foundation (2016T90552), and the Class General Financial Grant from the China Postdoctoral Science Foundation (2015M580527)

Background: The rostral anterior cingulate cortex (rACC) is important in pain expectation. Previous studies demonstrated that mechanical stimulus-induced withdrawal behaviors are spinally-mediated nocifensive reflexes in rats, but it is not known whether pain expectation is influenced by withdrawal behaviors.

Material/Methods: We reanalyzed previous mechanosensitivity measurements of 244 rats measured 5 times in succession. To study neural oscillation in the rACC, 1 recording microwire array was surgically implanted. Then, we simultaneously recorded the local field potential (LFP) of the rACC over the course of multiple withdrawal behaviors in unanesthetized rats.

Results: From our previous withdrawal behavioral data in 244 rats, we observed that the distributions of paw withdrawal thresholds (PWTs) were denser and more concentrated after the first withdrawal behavior. Compared to the first mechanical stimulus, increased neuronal synchrony and a stronger delta band component existed in each pre-stimulus LFP in the rACC during subsequent stimuli.

Conclusions: Pain expectation could be involved in withdrawal behaviors, which is related to increased total power and delta band power of the subsequent pre-stimulus LFPs in the rACC.

MeSH Keywords: Cognitive Science • Cone-Beam Computed Tomography • Gyrus Cinguli • Microelectrodes • Pain

Full-text PDF: http://www.medscimonit.com/abstract/index/idArt/903292

Indexed in: [Current Contents/Clinical Medicine] [SCI Expanded] [ISI Alerting System] [ISI Journals Master List] [Index Medicus/MEDLINE] [EMBASE/Excerpta Medica] [Chemical Abstracts/CAS] [Index Copernicus]

Background

Paw withdrawal thresholds (PWTs) is the most commonly used method to assess pain-related behaviors in rodents [1, 2]. Due to the absence of verbal communication with animals, pain cannot be monitored directly in preclinical research but can be estimated by examining behavioral responses to nociceptive stimuli [3]. Hence, a nociceptive withdrawal reflex response is used to explore pain mechanisms in rats [4]. However, pain is a subjective and multidimensional experience, including sensory-discriminative, affective, and cognitive components, which requires cortical involvement and modulation [5–7]. Previous studies have shown that spinal dorsal horn neurons receive nociceptive information, convey it to the ventral horn, and contribute to spinally-mediated nocifensive reflexes [8]. If the mechanical stimulus-induced withdrawal behavior is only a simple reflex that does not activate cortical areas, the PWTs cannot be used as a behavioral standard for evaluating pain. Thus, it is crucial to establish whether a synchronous cortical response accompanies the withdrawal behavior used in preclinical pain research.

Emerging evidence suggests that cortical areas are adaptive processors, subject to top-down expectations, in which neural activity reflects internal goals and states in addition to external stimuli [9]. The rostral anterior cingulate cortex (rACC, Brodmann's areas 24 and 32) [10,11], a major area implicated in the descending pain modulatory system [12], is also involved in prefrontal top-down processing [13]. Previous research, using positron emission tomography (PET), documented that rACC served to prepare for upcoming pain by regulating anticipatory threat responses [14], consistent with activity in the rACC during visual stimuli predicting disagreeable noises observed in an fMRI study [15].

Expectation is highly subjective and subject to the intrinsic dynamics of oscillations and synchrony in cognitive processing. Neural oscillations observed in local field potentials (LFPs) reflect coherent neuronal population activity. The mechanisms of oscillation generation are computationally interesting and may serve as a means of explaining various aspects of perception and cognition [9] . Therefore, our key interest in this study was to simultaneously record the LFPs of the rACC in quietly resting, unanesthetized rats under multiple mechanical stimulus conditions to elucidate pain expectation modulation coincident with the withdrawal behaviors.

Material and Methods

Animals

Male adult Sprague-Dawley rats, 250–300 g body weight, were obtained from the Experimental Animal Center of Zhejiang Chinese Medical University. The animals were housed in groups of 5 in plastic cages with soft bedding at the University Animal Care facility with an artificial 12/12 h light-dark cycle (lights on at 8 a.m.). Animals received food and water ad libitum with a constant room temperature of 23–25°C and a relative humidity of 40–70%. Before experimental manipulations, rats were given a period of 1 week to adjust to the new surroundings. The whole experiment was performed in accordance with the guidelines of the International Association for the Study of Pain and the Institutional Animal Ethics Committee (IAEC).

Nociceptive behavioral testing

Mechanical hyperalgesia is the criterion standard in nociceptive behavioral testing. The paw withdrawal threshold was measured automatically using a dynamic plantar aesthesiometer (model 37450; Ugo Basile, Comerio, Italy). Animals were habituated to the testing surroundings daily for 2 consecutive days (between 9 a.m. and 12 a.m.) before testing. The room temperature and humidity remained stable during testing. Each rat moved freely in a transparent plastic compartment of a 6-compartment box with a wire mesh floor and were acclimatized for 20 min before the test session. A paw-flick response was elicited by applying an increasing vertical force (increased steadily from 0 to 50 grams in 20 s) using a stainless-steel probe (a straight 0.5-mm diameter) placed underneath the mesh floor and focused on the middle of the plantar surface of the ipsilateral hind paw. The ipsilateral paw of each rat was measured 5 times at intervals of 1-min or more and the value of the applied force was determined and used for statistical analysis. All manipulations were performed under the guidance of an operator. The operator was blind to the experimental conditions.

Surgical procedures

To study electrophysiological properties, 1 recording microwire array was surgically implanted under urethane anesthesia (1.2 g/kg i.p., Sigma-Aldrich, USA). Surgical procedures were the same as in previous studies [16,17], with the exception of the location of the microwires arrays. Rats were placed in a stereotaxic frame on a heated surgical platform maintained at a constant temperature of 37°C, and a midline scalp incision was made to expose the skull to allow the implantation of 4 screws and an array. The screws were applied for grounding purposes. The array was driven into the right side rACC at a 20-degree angle using a hydraulic microdrive (model 51421, Stoelting, Wood Dale, USA); the array was advanced while recording the neural ensemble activity to achieve the correct placement. Each microwire array consisted of 8 filaments of nickel chromium wire (35-μm diameter, Stablohm 675; California Fine Wire Company, Grover Beach, CA, USA). The array was constructed in 4×2 architecture, with 200 μm

Indexed in: [Current Contents/Clinical Medicine] [SCI Expanded] [ISI Alerting System] [ISI Journals Master List] [Index Medicus/MEDLINE] [EMBASE/Excerpta Medica] [Chemical Abstracts/CAS] [Index Copernicus]

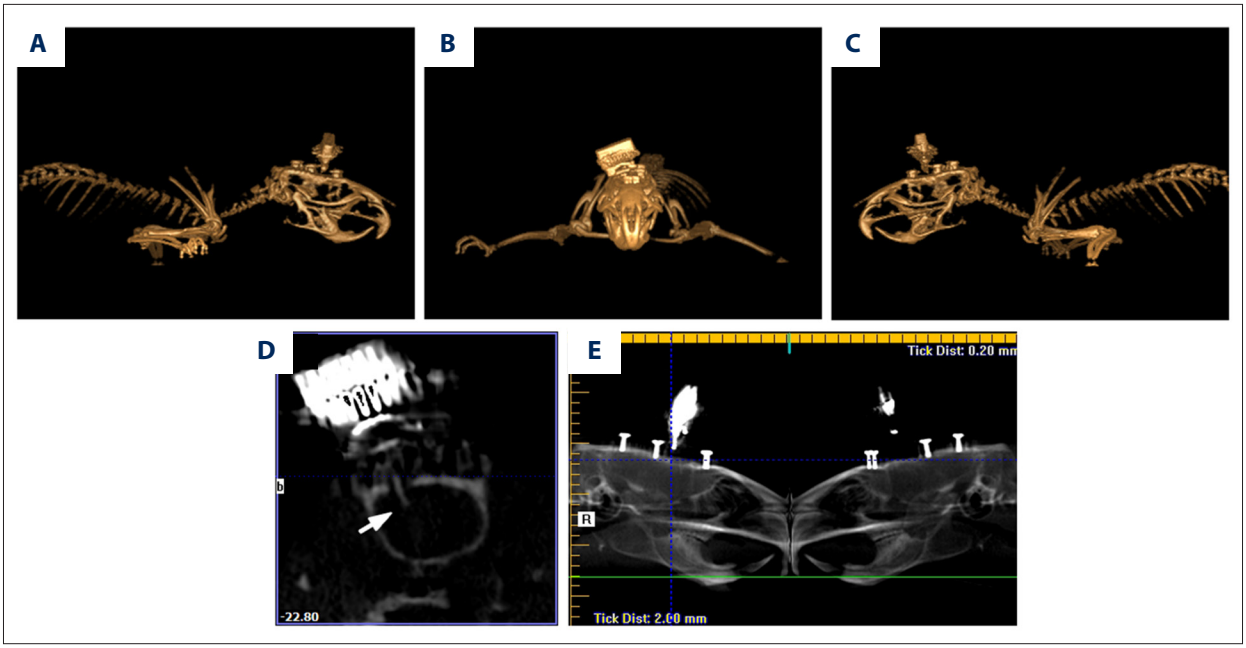

Figure 1. Localization of implanted microwire array is confirmed in the rACC using three-dimensional reconstructions and radiographs from CBCT. (**A**) Right lateral view. (**B**) Anterior-posterior view. (**C**) Left lateral view. (**D**) The cross-section of the rACC showing implant placement (arrow). (**E**) Reconstructed panoramic radiograph. rACC – rostral anterior cingulate cortex; CBCT – cone-beam computed tomography.

between recording wires. The following coordinates (relative to the bregma) were used to center the array: rACC (+2.7 mm rostrocaudal, +0.8 mm mediolateral, 2.0 mm dorsoventral). Animals were placed in a new cage with warm bedding until awakening from anesthesia. After a 7-day recovery period, rats were allowed to adapt to the recording environments (nociceptive behavioral testing surroundings) for 2 days.

Localization of implanted microwire arrays

With the application of cone-beam computed tomography (CBCT), we could evaluate the location of microwire array more accurately (Figure 1), since CBCT image data are acquired in digital format from a single 360° rotational scan and through a KaVo CT 3D examination (KaVo, Germany) with 0.2-mm voxel size. We performed 3D modeling and panoramic reconstructions, as well as cross-sections obtained using reconstruction software (eXamVision, Version 1.9.3.13, Kavo Dental, Germany). This technique allowed immediate identification of the recording site during implantation surgery.

Neural recordings

Extracellular local field potentials (LFPs) were recorded from the implanted microwire array by a Cerebus Neural Signal Processing system (Blackrock Microsystems, Salt Lake City, UT, USA). LFPs signals were preamplified (300×), bandpass filtered (0.3–250 Hz), and sampled at 1 KHz. Neural recordings were obtained in the nociceptive behavioral testing environments during quiet states. A plantar video camera and video tracking system (ANY-maze, Stoelting, CO, USA) was used to provide real-time imaging of the rats' plantar and the stimulus probe in the dynamic plantar aesthesiometer, permitting synchronization of the probe's stimulus process with the acquired neuronal data. No animals were removed from the study due to poor placement of the recording wires.

Data analysis

Behavioral data

Data from previous mechanosensitivity tests in 244 rats were reanalyzed. Paw withdrawal thresholds to 5 sequential mechanical stimuli were expressed as a scatter plot and violin plot (Figure 2). The scatter plot was an important tool for assessing the trend shown by the data; it represents each observation as a point, with paw withdrawal threshold plotted on the y-axis. The violin plot was a combination of a box plot and a kernel density plot, which retained more information about the shape of the distribution. The main advantage of the violin plot was that it presented the density; a wider violin plot shows higher density. Both types of plots were generated using the ggplot2 R package [18].

Levene's test was used to assess the homogeneity of variances across samples. A small *P* value of Levene's test (typically

Indexed in: [Current Contents/Clinical Medicine] [SCI Expanded] [ISI Alerting System] [ISI Journals Master List] [Index Medicus/MEDLINE] [EMBASE/Excerpta Medica] [Chemical Abstracts/CAS] [Index Copernicus]

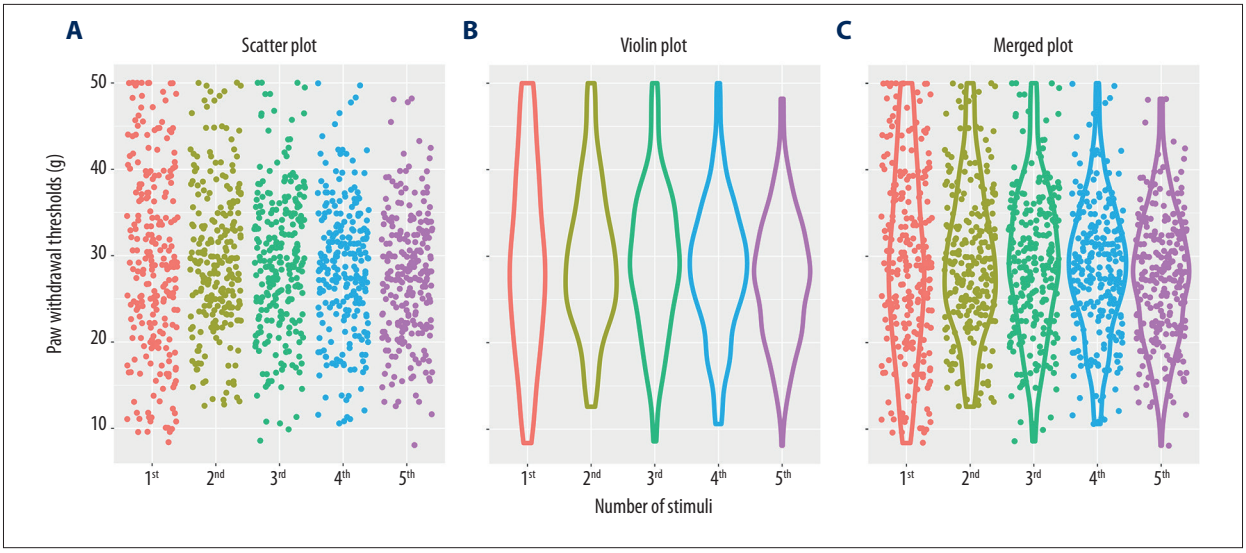

Figure 2. Individual paw withdrawal thresholds to mechanical stimuli of previous mechanosensitivity measurements in 244 rats. (**A**) Scatter plots illustrate the distribution of withdrawal threshold values, where each dot represents a withdrawal threshold. (**B**) Violin plots reveal the heterogeneity in the population by visualizing the density of withdrawal threshold values at each time. (**C**) Merged plots of scatter plots and violin plots.

0.05) suggests that differences in sample variances were unlikely to have resulted from random sampling from populations with equal variances, leading to rejection of the hypothesis that the variances were homogenous.

Spectral analysis

Data were processed and validated by offline analysis using NeuroExplorer 5.021 (NEX, Plexon Inc.) and exported to MatLab 2014a (MathWorks, Natick, MA) for complementary analysis.

Spectrogram analysis was used to visualize LFP power at different frequency bands as a function of time for each condition. The raw rACC LFPs were bandpass filtered at 2–45 Hz using a non-causal zero-phase-shift filter (fourth-order Butterworth). Next, the power spectral densities (PSD) were calculated by Hanning window, 2^{10} frequency bins over the 2-45 Hz range, and 50% overlapping windows. The power was normalized by the logarithm of the PSD (in decibels) and a smoothing was applied (Gaussian filter, width=3). Five frequency band intervals were considered: 2–4 Hz (delta), 4–9 Hz (theta), 9–15 Hz (alpha), 15–30 Hz (beta), and 30–45 Hz (gamma).

Statistical analysis

All data for parametric analysis was originally assessed using Levene's test for homogeneity of variance. One-way or two-way repeated measures analysis of variance (rmANOVA) with Bonferroni post hoc analysis was used when the variances were equal. When the variance was not homogeneous, Dunnett's T3 post hoc test was used to perform pairwise comparisons. In all cases, results were considered to be statistically significant at $p<0.05$.

Results

Withdrawal behaviors during each measurement

We reanalyzed 1220 previous mechanosensitivity measurements on the ipsilateral paws of 244 rats measured 5 times in succession. We assessed homogeneity of variance using Levene's test before statistical procedures were applied. Variances were not equal across all 5 successive measurements (Levene statistic=14.136, df1=4, df2=1215, $p<0.001$). However, this was due entirely to the first measurement; the variances of the subsequent 4 measurements were homogeneous (Levene statistic=1.769, df1=3, df2=972, $p=0.151$). Pairwise comparisons using Dunnett's T3 post hoc test found no significant differences among the 5 sequential measurements. In Figure 2, the scatter and violin plots illustrate the shape and density of the distributions. These results suggest that during 4 later measurements, the distributions of PWTs were more robust and volatility was smaller than in the first one.

Pre-stimulus LFP activity of the rACC during each measurement

Compared to the first mechanical stimulus, higher-amplitude LFP signals were observed during the pre-stimulus period of the subsequent 4 stimuli (Figure 3A), yielding a generally higher PSD in the longitudinal heat maps (Figure 3B). The pre-stimulus PSD

Indexed in: [Current Contents/Clinical Medicine] [SCI Expanded] [ISI Alerting System] [ISI Journals Master List] [Index Medicus/MEDLINE] [EMBASE/Excerpta Medica] [Chemical Abstracts/CAS] [Index Copernicus]

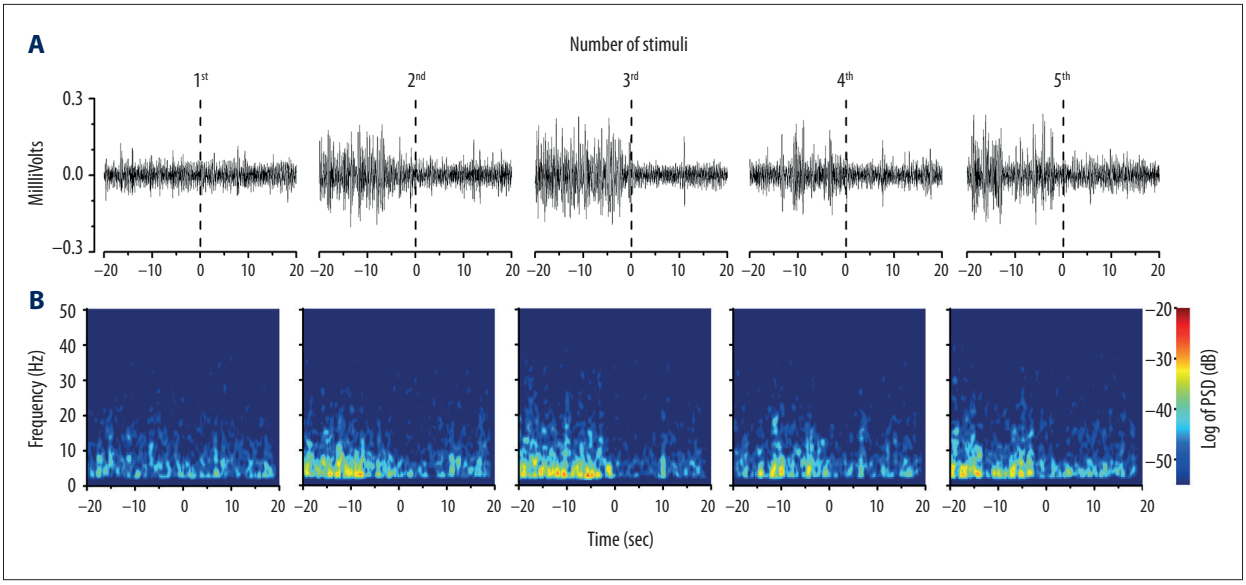

Figure 3. Mechanical stimulus-induced oscillatory activity of the rACC during each successive stimulus. (**A**) Representative examples of spontaneous LFP recordings (band pass filtered between 2 and 45 Hz). (**B**) Spectrograms of the same LFP signals as in (**A**). The power was normalized by the logarithm of the PSD (in decibels) within the frequency range (2–45 Hz). The inspection of amplitude (**A**) and PSD (**B**) indicated higher pre-stimulus LFP amplitudes preceding the last four stimuli relative to the first. rACC – rostral anterior cingulate cortex; LFP – local field potential; PSD – power spectral density.

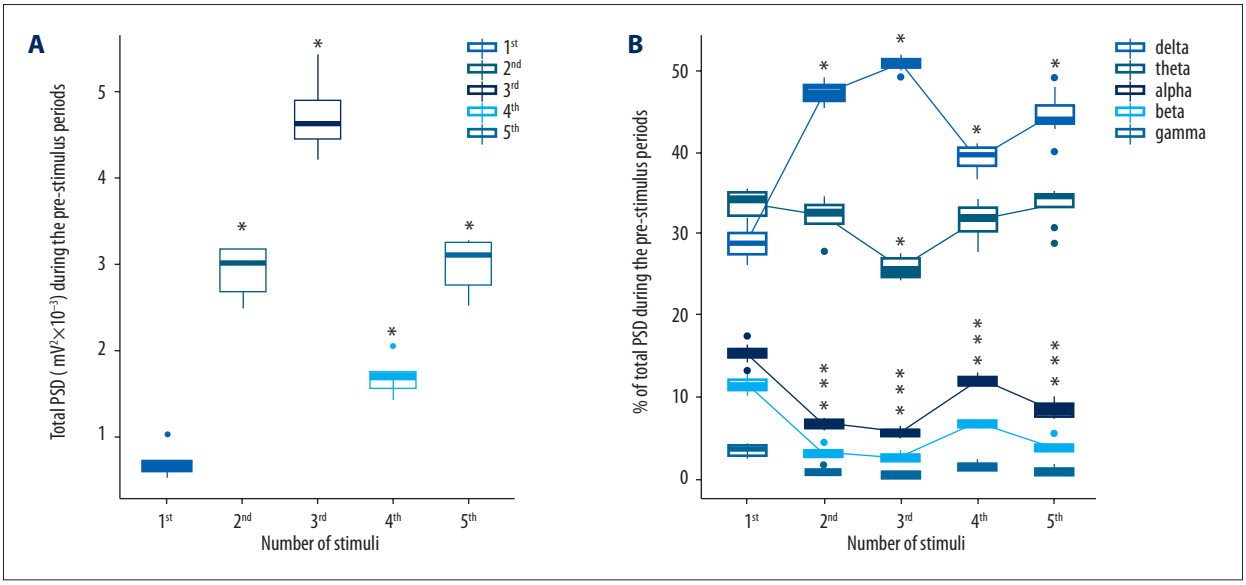

Figure 4. The PSD of LFPs within the frequency range analyzed (2–45 Hz) for rACC LFP signals, comparing the 1st and later stimuli. (**A**) Raw total PSD in the pre-stimulus periods. (**B**) The PSD was normalized by the percentage of total power in five frequency bands in the pre-stimulus periods. Five frequency band intervals were considered: 2–4 Hz (delta), 4–9 Hz (theta), 9–15 Hz (alpha), 15–30 Hz (beta), and 30–45 Hz (gamma). Comparisons between the 1st and later stimuli are based on one-way rmANOVA (**A**) and two-way rmANOVA (frequency bands × number of stimuli) (**B**), followed by a post hoc Bonferroni test. * $P<0.001$. The inspection of PSD (**B**) indicated a stronger delta band component was present in the last four stimulus presentations. PSD – power spectral density; LFPs – local field potentials; rmANOVA – repeated measures analysis of variance.

of LFP signals is further shown in Figure 4A and 4B. The statistical comparison of the total PSD of each pre-stimulus period across the 5 sequential stimuli revealed significant differences (one-way rmANOVA; $F[4,35]= 246.6$, $p<0.001$). The pre-stimulus total PSD of the last 4 stimuli was significantly higher than that of the first stimulus ($p<0.001$, $p<0.001$, $p<0.001$, $p<0.001$)

Indexed in: [Current Contents/Clinical Medicine] [SCI Expanded] [ISI Alerting System] [ISI Journals Master List] [Index Medicus/MEDLINE] [EMBASE/Excerpta Medica] [Chemical Abstracts/CAS] [Index Copernicus]

(Figure 4A). Furthermore, during the pre-stimulus period, significant differences were encountered across frequency bands (two-way rmANOVA; F[4,140]=4739.22, $p<0.001$) and the number of stimuli (two-way rmANOVA; F[4,140]=102.50, $p<0.001$; Figure 4B). Compared to the first pre-stimulus period, post hoc analysis revealed an increase in PSD in the delta frequency band ($p<0.001$ for the subsequent 4 times), and a decrease in the theta band ($p<0.001$ for the third time), as well as in the alpha, beta, and gamma bands ($p<0.001$, $p<0.001$, and $p<0.001$ for the subsequent 4 times). Together, these data suggest that paw withdrawal behavior increased the total power and delta band power of the pre-stimulus LFPs in the rACC during subsequent stimuli.

Discussion

In previously published studies, PWTs were generally measured multiple times, and the arithmetical average was used to assess mechanical hyperalgesia in rats. This view is built on the assumption that the paw withdrawal behavior is nothing more than a spinal reflex; therefore, the method of averaging multiple measures in physics was deemed valid in living animals with perceptual ability. Our results indicate that a top-down expectation is manifested by changes in pre-stimulus LFP activity in the rACC over the course of multiple withdrawal behaviors. In the dataset of withdrawal behaviors, the distributions of PWTs in the subsequent 4 measurements were denser and more stable than in the first one. Taken together, our measurements during paw withdrawal are indicative of cognitive processing of pain, as exemplified by changes in the rACC LFP activity in the pre-stimulus period, and expectations increase the stability of later withdrawal behaviors.

The LFP, measured with very fine microwires, reflects the synaptic activity of only tens to perhaps thousands of nearby neurons. Power increase is usually interpreted as increased synchrony in the neuronal assembly surrounding each microwire, implying the connectivity between these neurons [19]. Our results are in agreement with the recent characterization of the brain as a "dynome" [20] or "chronectome" [21], highlighting the role of dynamic communication within or between networks in shaping cognition and behavior. As Aaron and Karen reported, the processing of pain is encoded by a "pain connectome" [22], the spatiotemporal signature of brain network communication that represents the integration of all cognitive, affective, and sensorial aspects of pain. Additionally, a strong delta band component was encountered during pre-stimulus periods of the last 4 withdrawal behaviors. In fact, it has been shown that the pre-stimulus modulation of delta oscillations serves as a neural mechanism underlying the faster processing of expected events [23]. Our results recorded during multiple withdrawal stimuli also confirm an increase of the delta band power, which is correlated with an increase in top-down expectations, inducing more stable withdrawal behaviors.

Another important point is that the method of averaging multiple measures in physics cannot be directly used in the detection of PWTs. Previous research of pain in rodents has usually treated PWTs as a key index of pain behavior in the study of pain-related molecular targets, while only a few of these targets play an important role in humans. The reason for this may be that the PWTs is not equivalent to pain threshold, defined as "the minimal intensity of a stimulus that is perceived as painful" [24]. Pain perception needs the involvement of cortical areas. Our results show that the pre-stimulus period of the last 4 withdrawal responses exhibited a change in cortical activity and brain state. Taken together, these results suggest that the average PWT, under conditions of cortical engagement, might be regarded as a behavioral indicator of pain in rats. Therefore, the results may be conducive to the translation from basic research of pain-related biomarkers to potential clinical applications.

Conclusions

This study provides evidence that the first withdrawal behavior causes changes of pre-stimulus LFP activity in the rACC during subsequent stimuli, and this preparation in advance could affect subsequent stimuli-induced withdrawal behaviors, which contribute to the dynamics of bottom-up input and top-down expectation.

Conflict of Interest

None.

References:

1. Du JY, Fang JQ, Liang Y et al: Electroacupuncture attenuates mechanical allodynia by suppressing the spinal JNK1/2 pathway in a rat model of inflammatory pain. Brain Res Bull, 2014; 108: 27–36
2. Kwon SG, Yoon SY, Roh DH et al: Peripheral neurosteroids enhance P2X receptor-induced mechanical allodynia via a sigma-1 receptor-mediated mechanism. Brain Res Bull, 2016; 121: 227–32
3. Le Bars D, Gozariu M, Cadden SW: Animal models of nociception. Pharmacol Rev, 2001; 53: 597–652
4. Mogil JS: Animal models of pain: Progress and challenges. Nat Rev Neurosci, 2009; 10: 283–94
5. Barrot M: Tests and models of nociception and pain in rodents. Neuroscience, 2012; 211: 39–50
6. Rainville P, Carrier B, Hofbauer RK et al: Dissociation of sensory and affective dimensions of pain using hypnotic modulation. Pain, 1999; 82: 159–71

Indexed in: [Current Contents/Clinical Medicine] [SCI Expanded] [ISI Alerting System] [ISI Journals Master List] [Index Medicus/MEDLINE] [EMBASE/Excerpta Medica] [Chemical Abstracts/CAS] [Index Copernicus]

7. Salomons TV, Moayedi M, Erpelding N et al: A brief cognitive-behavioural intervention for pain reduces secondary hyperalgesia. Pain, 2014; 155: 1446–52
8. Todd AJ: Neuronal circuitry for pain processing in the dorsal horn. Nat Rev Neurosci, 2010; 11: 823–36
9. Arnal LH, Giraud AL: Cortical oscillations and sensory predictions. Trends Cogn Sci, 2012; 16: 390–98
10. Dreher JC, Grafman J: Dissociating the roles of the rostral anterior cingulate and the lateral prefrontal cortices in performing two tasks simultaneously or successively. Cereb Cortex, 2003; 13: 329–39
11. Navratilova E, Xie JY, Meske D et al: Endogenous opioid activity in the anterior cingulate cortex is required for relief of pain. J Neurosci, 2015; 35: 7264–71
12. Jensen KB, Kosek E, Petzke F et al: Evidence of dysfunctional pain inhibition in Fibromyalgia reflected in rACC during provoked pain. Pain, 2009; 144: 95–100
13. Petrovic P, Kalso E, Petersson KM et al: A prefrontal non-opioid mechanism in placebo analgesia. Pain, 2010; 150: 59–65
14. Wager TD, Scott DJ, Zubieta JK: Placebo effects on human mu-opioid activity during pain. Proc Natl Acad Sci USA, 2007; 104: 11056–61
15. Buchel C, Morris J, Dolan RJ et al: Brain systems mediating aversive conditioning: An event-related fMRI study. Neuron, 1998; 20: 947–57
16. Cardoso-Cruz H, Lima D, Galhardo V: Impaired spatial memory performance in a rat model of neuropathic pain is associated with reduced hippocampus-prefrontal cortex connectivity. J Neurosci, 2013; 33: 2465–80
17. Cardoso-Cruz H, Sousa M, Vieira JB et al: Prefrontal cortex and mediodorsal thalamus reduced connectivity is associated with spatial working memory impairment in rats with inflammatory pain. Pain, 2013; 154: 2397–406
18. Wickham H: Ggplot2: Elegant graphics for data analysis. New York: Springer, 2009
19. Buzsáki G: Rhythms of the brain. Oxford; New York: Oxford University Press, 2006
20. Kopell NJ, Gritton HJ, Whittington MA et al: Beyond the connectome: The dynome. Neuron, 2014; 83: 1319–28
21. Calhoun VD, Miller R, Pearlson G et al: The chronnectome: Time-varying connectivity networks as the next frontier in fMRI data discovery. Neuron, 2014; 84: 262–74
22. Kucyi A, Davis KD: The dynamic pain connectome. Trends Neurosci, 2015; 38: 86–95
23. Stefanics G, Hangya B, Hernadi I et al: Phase entrainment of human delta oscillations can mediate the effects of expectation on reaction speed. J Neurosci, 2010; 30: 13578–85
24. Loeser JD, Treede RD: The Kyoto protocol of IASP Basic Pain Terminology. Pain, 2008; 137: 473–77

Indexed in: [Current Contents/Clinical Medicine] [SCI Expanded] [ISI Alerting System] [ISI Journals Master List] [Index Medicus/MEDLINE] [EMBASE/Excerpta Medica] [Chemical Abstracts/CAS] [Index Copernicus]